Title
Atomic chlorine concentrations derived from ethane and hydroxyl measurements over the equatorial Pacific Ocean: Implication for dimethyl sulfide and bromine monoxide

Journal
Journal of Geophysical Research D: Atmospheres, 110(20)

ISSN
0148-0227

Authors
Wingenter, OW
Sive, BC
Blake, NJ
et al.

Publication Date
2005-10-27

DOI
10.1029/2005JD005875

Atomic chlorine concentrations derived from ethane and hydroxyl measurements over the equatorial Pacific Ocean: Implication for dimethyl sulfide and bromine monoxide

Oliver W. Wingenter

Department of Chemistry and the Geophysical Research Center, New Mexico Institute of Mining and Technology, Socorro, New Mexico, USA

Barkley C. Sive

Climate Change Research Center–Institute for the Study of Earth, Oceans, and Space (CCRC-ISEOS), University of New Hampshire, Durham, New Hampshire, USA

Nicola J. Blake, Donald R. Blake, and F. Sherwood Rowland

Department of Chemistry, University of California, Irvine, California, USA

Received 12 February 2005; revised 18 April 2005; accepted 10 May 2005; published 29 October 2005.

[1] Atomic chlorine and bromine monoxide concentrations ([Cl] and [BrO]) and dimethyl sulfide (DMS) sea-air fluxes are estimated from data collected during a Lagrangian flight made near Christmas Island (2°N, 157°W) during August 1996 aboard the NASA P3-B aircraft. Intensive hydrocarbon sampling began in the surface layer (SL) one-half hour after sunrise and continued until ~1300 local solar time. Our empirical model includes in situ observations of hydroxyl [HO] and precise measurements of ethane (C_2H_6) mixing ratios. Ethane was ~40 pptv higher in the buffer layer (BuL) than in the SL, thus vertical exchange tended to replace any C_2H_6 that was photochemically removed in the SL. In spite of this, SL C_2H_6 mixing ratios decreased significantly during the flight. Using only the measured [HO] and estimated vertical mixing, our mass balance equation cannot explain all of the observed SL C_2H_6 loss. However, when an initial [Cl] of 8.4 (±2.0) × 10^4 Cl cm^{-3}, decreasing to 5.7 (±2.0) × 10^4 Cl cm^{-3} at midday, is included, the observed and estimated C_2H_6 values are in excellent agreement. Using our [Cl], we estimate a DMS flux a factor of 2 higher than when HO is the only oxidant considered. This flux estimate, when compared to that derived by Lenschow et al. (1999), suggests that if the differences are real, we may be missing a loss term. Best agreement occurs when an average BrO mixing ratio of 1.3 (±1.3) pptv is included in our mass balance equation.

Citation: Wingenter, O. W., B. C. Sive, N. J. Blake, D. R. Blake, and F. S. Rowland (2005), Atomic chlorine concentrations derived from ethane and hydroxyl measurements over the equatorial Pacific Ocean: Implication for dimethyl sulfide and bromine monoxide, *J. Geophys. Res.*, *110*, D20308, doi:10.1029/2005JD005875.

1. Introduction

[2] Atomic chlorine (Cl), a radical species, is a powerful oxidant reacting with many volatile organic compounds at rates approaching the collisional limit. Because much of the Cl in the atmosphere originates from reactions involving sea salt aerosol [e.g., *Rossi*, 2003; *Finlayson-Pitts*, 2003], Cl is expected to be at its highest concentration in the marine boundary layer (MBL) [*Singh and Kasting*, 1988; *Platt et al.*, 2004]. Therefore Cl should be an important oxidant in the MBL for those trace gases that react quickly with Cl. For example, DMS reacts about 60 times faster with Cl than with HO [*Stickel et al.*, 1992; *Sander et al.*, 2002].

[3] Because of its low abundance and high reactivity, [Cl] cannot be measured directly with present instrumentation and has only been characterized in a few field experiments in the MBL using observation of nonmethane hydrocarbons and halocarbons, while simultaneously solving for air mass mixing and [HO] [*Singh et al.*, 1996; *Wingenter et al.*, 1996, 1999]. During polar sunrise, a different approach employing nonmethane hydrocarbons and their reactivities to Cl and Br yielded average [Cl] and [Br] estimated over a few days [*Jobson et al.*, 1994; *Ariya et al.*, 1998; *Ramacher et al.*, 1999]. Bromine monoxide (BrO) has been characterized by atomic resonance fluorescence during Arctic sunrise [*Avallone et al.*, 2003]. *Hausmann and Platt* [1994] also quantified BrO in the Arctic region using differential optical absorption spectroscopy (DOAS). This technique has been used to measure chlorine monoxide (ClO) and BrO near large dry salt lake beds [*Hebestreit et al.*, 1999; *Stutz et al.*, 2002]. Balloon-mounted DOAS instruments have measured a tropospheric average background BrO mixing ratio of 1–2 pptv [*Fitzenberger et al.*, 2000]. A wealth of knowledge of the distribution of BrO worldwide, especially in the polar regions, has been gained by DOAS instruments deployed on satellites [*Hegels et al.*, 1998;

0148-0227/05/2005JD005875

Wagner et al., 2001]. Mist chamber measurements of Cl* (the sum of Cl, Cl_2, ClO, HOCl) and HCl* (mostly HCl; hydrogen chloride) have been reported recently from an experiment in Hawaii [*Pszenny et al.*, 2004]. Measurement of unique products of isoprene oxidation by Cl in a coastal urban setting is another method to infer [Cl] [*Ragains and Finlayson-Pitts*, 1997; *Tanaka et al.*, 2003]. In situ measurements in the MBL, which utilized an atmospheric-pressure chemical ionization mass spectrometer [*Spicer et al.*, 1998], revealed high levels of Cl_2 in a coastal region.

[4] Measurements of [Cl] and [Br] in aerosols indicate that these halogen species were being depleted from sea salt particles [*Duce et al.*, 1963]. Several mechanisms have been shown to produce photolabile atomic chlorine precursors. Laboratory studies of reactions of NO_y (NO, NO_2, N_2O_5, HNO_3, etc.) with sea salt aerosol reveal the production of photochemically active chlorine species, and in some studies analogous active bromine species were produced. The NO_y and salt reactions generally proceed as

$$\text{(R1)} \qquad NO_{y(gas)} + NaCl_{(aq)} \rightarrow ZCl_{(gas)} + \text{products}$$

$$\text{(R2)} \qquad ZCl_{(gas)} + h\nu \rightarrow Cl + \text{products},$$

where *Z*Cl is an easily photolyzed Cl species, such as Cl_2, NOCl, $ClNO_2$, or HOCl, which can accumulate overnight and dissociate within about 1 hour after sunrise (for reviews see *Rossi* [2003], *Finlayson-Pitts* [2003], and *von Glasow and Crutzen* [2003]).

[5] Laboratory and modeling results [*Abbatt and Waschewsky*, 1998; *Fickert et al.*, 1999; *Vogt et al.*, 1996] indicate that the reactions of HOCl and HOBr are important in releasing chloride and bromide from sea-salt aerosol,

$$\text{(R3)} \qquad HOX_{(gas)} + Cl^-_{(aq)} + H^+_{(aq)} \rightarrow XCl_{(gas)} + H_2O_{(l)}.$$

Here X is either a Cl or Br atom.

[6] Atmospheric HO can react with chloride (Cl^-) on sea salt aerosol surfaces generating Cl_2 in the gas phase [*Oum et al.*, 1998; *Knipping et al.*, 2000].

$$\text{(R4)} \qquad 2HO_{(gas)} + 2Cl^-_{(Surface)} \rightarrow 2(HO.Cl^-)_{(Surface)} \rightarrow Cl_{2(gas)} + 2(HO^-)_{(Surface)}.$$

This reaction sequence, followed by fast photolysis, produces Cl diurnal profiles similar to HO [*Knipping et al.*, 2000]. By including this reaction in an atmospheric model, *Knipping et al.* [2000] were able to reproduce field results [*Wingenter et al.*, 1996, 1999] well.

[7] Another process that recycles Cl and mimics the HO diurnal cycle is

$$\text{(R5)} \qquad HCl + HO \rightarrow Cl + H_2O.$$

Hydrogen chloride is the largest reservoir of inorganic Cl and is generated when Cl abstracts a hydrogen atom from an organic molecule, usually methane (CH_4). Because the recycling of Cl via (R5) is relatively slow, formation of HCl is considered a sink of Cl. Acidified aerosols also generate gas phase HCl. In the clean marine environment, the acid source is derived from the oxidation of DMS, which can form sulfuric acid (H_2SO_4). Subsequent accumulation of H_2SO_4 on sea-salt aerosol decreases aerosol pH. These processes lead to chloride and bromide deficits observed in marine aerosols [*Duce et al.*, 1963; *Keene et al.*, 1990].

[8] Methane (CH_4) is an import greenhouse gas, and measurements of its carbon isotopes provide constraints on sources and loss processes. The oxidation of CH_4 leads to an enrichment of atmospheric $^{13}CH_4$. Moreover, oxidation by Cl has an order of magnitude greater kinetic isotope effect than loss by HO [*Cantrell et al.*, 1990; *Saueressig et al.*, 1995, 2001; *Tyler et al.*, 2000] Ratios of $^{13}CH_4/^{12}CH_4$ that cannot be explained without including removal of CH_4 by Cl have been observed in the extratropical Southern Hemisphere [*Platt et al.*, 2004].

[9] Chlorine chemistry can initiate increased radical chemistry in coastal urban areas, such as southern California and Houston, Texas [*Knipping and Dabdub*, 2003; *Tanaka et al.*, 2003], and causes greater oxidation of volatile organic carbon species (VOCs). This can result in an increased rate of formation of two chief urban pollutants, ozone and organic aerosol. Reaction of Cl with hydrocarbons in the Arctic also leads to enhanced radical production [*Sander et al.*, 1997; *Wingenter et al.*, 2003], thereby fueling local photochemistry.

[10] The air-sea flux of dimethyl sulfide provides much of the sulfur to the natural atmosphere [*Bates et al.*, 1987b; *Charlson et al.*, 1987; *Chin et al.*, 2000] and is produced by phytoplankton [*Keller et al.*, 1989] and during the grazing of phytoplankton by microzooplankton [*Archer et al.*, 2001]. DMS can be oxidized to form new particles or to contribute to the growth of existing particles [*Davis et al.*, 1999; *von Glasow and Crutzen*, 2004]. In the unpolluted marine environment, sulfur from the sea-air flux of DMS is a major source of cloud condensation nuclei (CCN) [*Clarke et al.*, 1998]. Production and growth of CCN resulting from DMS oxidation is important in the remote MBL because it modifies cloud cover and planetary albedo, thus altering the radiative properties of the Earth [*Bates et al.*, 1987a; *Charlson et al.*, 1987; *Wingenter et al.*, 2004]. Therefore, understanding its photochemical loss processes and accurately determining its sea-air flux are essential to understanding current, past, and future climates.

[11] In this paper we employ time series observations of C_2H_6 and in situ measurements of HO concentrations made during a Lagrangian flight to estimate the [Cl] time series and DMS air-sea flux using empirical mass balance approaches. (In a Lagrangian reference frame, there is no relative motion between that which is being observed and the observer. Oftentimes mixing must be parameterized in a Lagrangian reference frame to obtain meaningful results [*Wingenter et al.*, 1996; *Davis et al.*, 1999].) The difference between this DMS sea-air flux estimate and that made using a micro-meteorological approach [*Lenschow et al.*, 1999] can be resolved if loss of DMS by BrO oxidation is included in a mass balance equation. The estimated values of [Cl] are employed in the New Mexico Tech/Georgia Tech (NMT/GT) photochemical point, or zero-dimensional, model in order to approximate the partitioning of inorganic Cl species in the gas phase, which may be helpful in planning future in situ measurements of these compounds.

2. Experimental

[12] In situ measurements of HO, DMS, and other chemical and physical parameters [*Mauldin et al.*, 1999; *Davis et al.*, 1999; *Hoell et al.*, 1999] were made aboard the P-3B

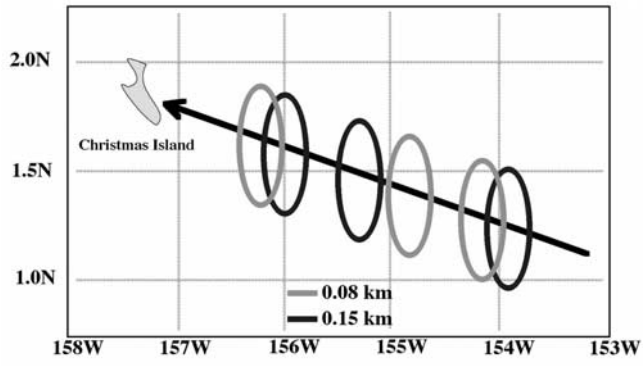

Figure 1. Flight path of the NASA P-3B during flight 7. The aircraft was flown in a Lagrangian manner in order to advect with the same air mass near Christmas Island. The flight legs below 200 m were used in this analysis. The figure is not drawn to scale. The shape of the flux circles in the figure are drawn as ellipses to emphasize that the air mass was advecting. (Adapted from *Davis et al.* [1999].)

aircraft during the NASA Global Tropospheric Experiment (GTE) Pacific Exploratory Mission (PEM) Tropics A field campaign near Christmas Island (2°N, 157°W) on 24 August 1996. One hundred and twenty whole air samples were also collected and analyzed for concentrations of nonmethane hydrocarbons, halocarbons, and alkyl nitrates [*Blake et al.*, 1999]. Limits of detection were $1-2 \times 10^5$ HO cm^{-3} for HO, 2 pptv for DMS, and 3 pptv for C_2H_6. The measurement precision for DMS and C_2H_6 was 2%. The precision of the individual DMS and C_2H_6 measurements was estimated by dividing the standard deviations of the measurements taken during a flux circle by the average mixing ratio. Thus our precision estimates include the natural variability of the air mass. Therefore this is an upper limit of the actual measurement precision. The flight data, including the merged data sets, are archived at www-gte.larc.nasa.gov/pem/pemta_dat.htm.

[13] The P-3B departed from Christmas Island (2°N, 158°W) just before dawn heading ESE to an air mass with a forecasted trajectory near Christmas Island at the time the flight would end (see Figure 1 of *Davis et al.* [1999]). The P-3B flew a series of six 0.5-hour surface layer (SL) flux circles below 200 m, advecting WNW in a Lagrangian manner (Figure 1). During each half hour flux circle, four to six whole air samples were collected, while approximately the same number of DMS samples were analyzed in situ by the research group from Drexel University [*Davis et al.*, 1999]. An intensively sampled ascent and descent to nearly 5 km were also made during the flight to obtain detailed vertical information regarding the chemical composition of this region (Figures 2 and 3). Details of this flight have been reported previously by *Davis et al.* [1999] and *Lenschow et al.* [1999].

3. Description of Calculations and Results

3.1. Empirical Box Models and Results

3.1.1. Atomic Chlorine

[14] Atomic chlorine concentrations as a function of time were determined using a mass balance equation for C_2H_6. Briefly, the change of concentration of a species, C in the

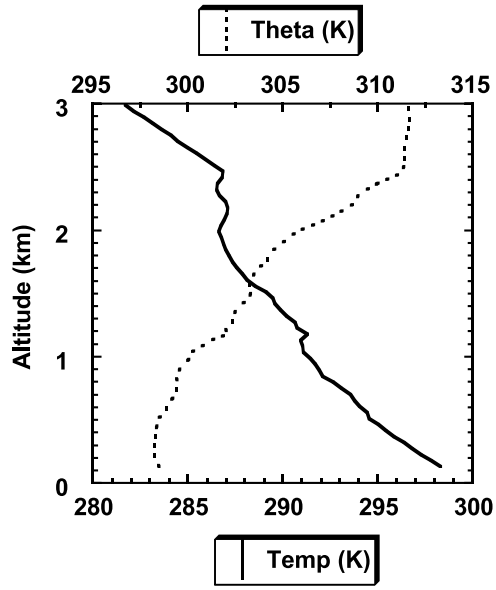

Figure 2. Temperature and potential temperature (theta; θ) versus altitude.

SL, with respect to time is equal to its production (P), minus loss (L), plus any change as a result of mixing with an air mass of different concentration (m),

$$d[C]_{SL}/dt = P - L + m, \quad (1)$$

Equation (1) can be written explicitly for C_2H_6 as

$$d[C_2H_6]_{SL}/dt = (k_{Cl+C2H6}[Cl] + k_{HO+C2H6}[HO])[C_2H_6] + (M/h)\left([C_2H_6]_{BuL} - [C_2H_6]_{SL}\right). \quad (2)$$

Equation (2) assumes that the marine source of ethane is negligible. The bimolecular rate constants for the reactions of Cl or HO with C_2H_6 [*Sander et al.*, 2002] are referred to

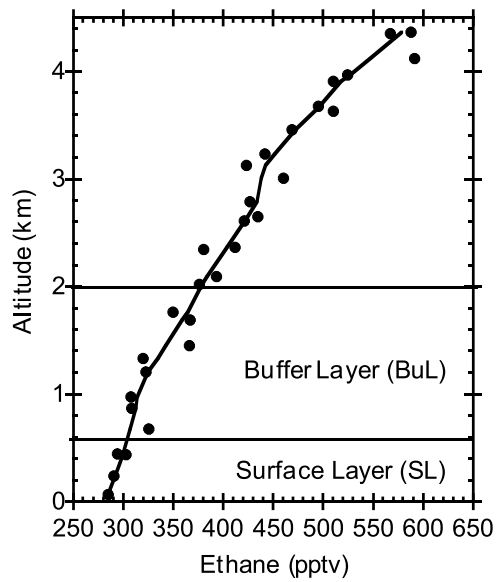

Figure 3. Ethane mixing ratios versus altitude.

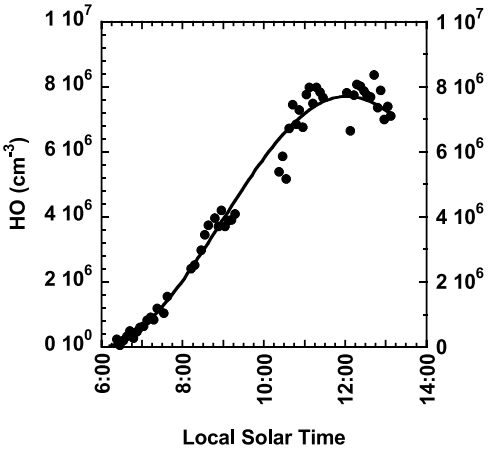

Figure 4. Measured HO concentrations versus local solar time in the surface layer.

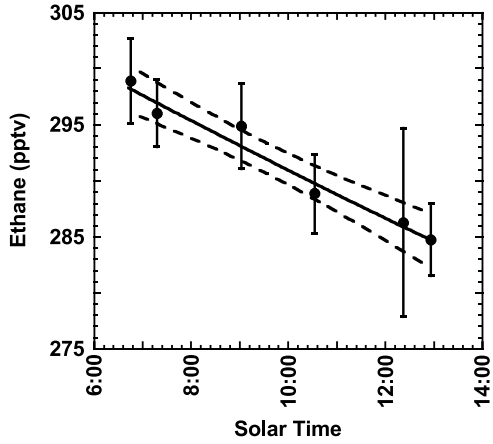

Figure 5. Ethane mixing ratio versus time. The data points are the average ethane mixing ratios for the samples taken during each circle below 200 m. The error bars are the standard deviation of the mean (stdeom) for each circle. Each data point was weighted based on the stdeom. The curve is the best-weighted linear least squares fit (R^2 = 0.97). The prediction intervals associated with the curve are at the 2-sigma level, meaning there is a 95% probability that the actual best linear fit should fall between the intervals.

as either $k_{Cl+C2H6}$ or $k_{HO+C2H6}$ and are 5.7×10^{-11} cm^3 molecule^{-1}s^{-1} for $k_{Cl+C2H6}$ and 2.4×10^{-13} cm^3 molecule^{-1}s^{-1} for $k_{HO+C2H6}$ at the average SL temperature, ~298 K, during this flight. The mixing parameter (M), of 1.2 ± 0.6 cm s^{-1}, was determined previously (G. Chen, personal communication, 2000) [*Davis et al.*, 1999]. The height of the SL (h) and the BuL were estimated from vertical profiles of Theta (potential temperature; θ) and temperature (T) measured during the ascent to nearly 5 km (Figure 2). Theta remained constant with height up to about 550 m, marking the top of the SL. The height of the BuL extended to approximately 1800 m where T remained fairly constant (until 2400 m) inhibiting mixing from the free troposphere. The difference in concentration of C_2H_6 in the BuL and SL is estimated from the mixing ratios observed during the ascent and descent occurring near 1000 local solar time (LST) (Figure 3). Concentrations of HO and C_2H_6 were taken from the best fit of their measured time series (Figures 4 and 5).

[15] The atomic chlorine concentration time series was formed by minimizing chi-square (X^2; see equation (3)) between measured [C_2H_6] and [C_2H_6] mixing ratios calculated using equation (2).

$$X^2 = \left([C_2H_6]_{observed} - [C_2H_6]_{estimated}\right)^2. \quad (3)$$

The calculated [Cl] time profile appears in Figure 6. The maximum calculated [Cl] of $8.4 \pm 2.0 \times 10^4$ Cl cm^{-3} occurs at the start of the Lagrangian experiment, which began about 0.5 hours after sunrise, decreasing about 30% to $5.7 \pm 2.0 \times 10^4$ Cl cm^{-3} at midday. The uncertainties are estimated by performing sensitivity studies and propagation of error estimates with nearly all of the uncertainty derived from M. The natural variation in C_2H_6 concentrations and analytical precision contributed negligibly to the error.

[16] An additional sensitivity analysis was performed by setting M equal to zero. This scenario suggests that even if no vertical replenishment of C_2H_6 had occurred, which seems highly unlikely given the observed vertical distribution of C_2H_6 and Theta, the levels of chlorine estimated in this scenario are still 31% of the estimate when mixing is considered. If no mixing had occurred, the empirical model suggests the average [Cl] over the 6-hour time period of 2×10^4 Cl cm^{-3}.

[17] The sea-air flux of C_2H_6 into the atmospheric surface layer in this region and during this flight was considered negligible and was not included in the calculations. The source of C_2H_6 to the MBL was from the free troposphere as evidenced by the C_2H_6 vertical profile (Figure 3). A significant marine flux of C_2H_6 would result in an underestimation of [Cl]. The concentrations of other measured hydrocarbons and halocarbons (i.e., propane, ethyne, C_2Cl_4, CH_4) were either too close to their detection limits or react too slowly with Cl to show significant change over the course of the observations, and therefore cannot be used in our mass balance analyses.

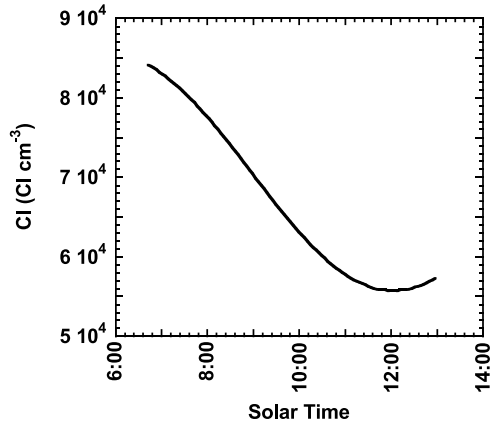

Figure 6. Chlorine mixing ratios versus time of day estimated from mass balance.

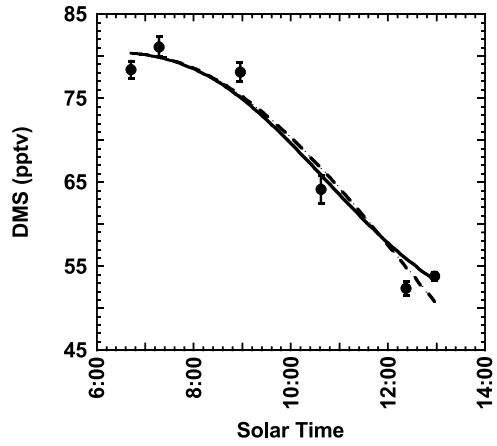

Figure 7. Measured and calculated DMS mixing ratios.

3.1.2. DMS Flux Estimate Including [Cl]

[18] The DMS flux was estimated using the calculated [Cl] time series (see above) and a mass balance equation,

$$d[DMS]_{SL}/dt = F/h + (k_{Cl+DMS}[Cl] + k_{HO+DMS}[HO])[DMS] + (M/h)\left([DMS]_{BuL} - [DMS]_{SL}\right). \quad (4)$$

The production term representing the sea-air flux of DMS is F divided by h. The Cl + DMS rate constant (3.3×10^{-10} cm^3 molecule^{-1}s^{-1}) used was determined by *Stickel et al.* [1992]. The reaction of chlorine with DMS can proceed by two channels. At low pressure, the hydrogen abstraction is important and results in the formation of HCl. At a pressure of ~203 torr the addition of Cl to DMS becomes important, resulting in a decreased HCl yield of ~0.5. At a pressure of 700 torr, the rate increases to 3.3×10^{-10} cm^3 molecule^{-1}s^{-1}. The atmospheric fate of the DMS-Cl adduct is uncertain [*Urbanski and Wine*, 1999], but in our analysis we assume that the addition channel is irreversible (I. Barnes, personal communication, 2004). The HO + DMS rate constant used was 5.0×10^{-12} cm^3 molecule^{-1}s^{-1} [*Sander et al.*, 2002]. The minimum in chi-square occurs when a constant DMS flux of 4.5 (±1.5) $\times 10^9$ DMS m^{-2}s^{-1} is used in the empirical model. The measured and empirically derived [DMS] time series are quite comparable, as shown in Figure 7.

3.1.3. DMS Flux Estimate Including Cl and BrO

[19] The difference between the DMS flux estimate of *Lenschow et al.* [1999], 6.1 (±1.9) $\times 10^9$ DMS m^{-2}s^{-1}, and our flux estimate (4.5 (±1.5) $\times 10^9$ DMS m^{-2}s^{-1}), which does not include loss of DMS by reacting with BrO, is used to estimate the concentration of BrO throughout the flight using a modified mass balance equation. It should be noted that the difference between the two flux estimates may not be significant. The mass balance equation now includes loss of DMS by BrO oxidation,

$$d[DMS]_{SL}/dt = F/h + (k_{Cl+DMS}[Cl] + k_{HO+DMS}[HO] + k_{BrO+DMS}[BrO])[DMS] + (M/h)\left([DMS]_{BuL} - [DMS]_{SL}\right). \quad (5)$$

The BrO + DMS rate constant used is from *Ingham et al.* [1999]. They report that the reaction proceeds with a rate constant of 4.4×10^{-13} cm^3 molecule^{-1}s^{-1} at our temperature of interest, 298 K, and the chief products are dimethyl sulfoxide (DMSO) and Br.

3.2. Photostationary State Point Model

[20] In order to investigate the gas phase partitioning of chlorine species, the New Mexico Tech/Georgia Tech (NMT/GT) photostationary state (PSS) point model was used. A version of the model has been described previously by *Davis et al.* [1996]. The updated version includes full $HO_x/NO_x/CH_4$/NMHC/Halogen chemistry. Chlorine chemistry is simulated using 46 mechanisms (Table 1). The NO instrument was not operational during flight 7. Model input for NO was treated similarly as by *Davis et al.* [1999] with NO mixing ratios of ~3 pptv and NO_x of 10 pptv measured by *Bradshaw et al.* [1999] during a DC-8 flight near Christmas Island 5 days later. Although, the PSS model does not explicitly incorporate aerosol reactions, it does include loss terms for washout/rainout and deposition.

[21] Output of our PSS model was informally compared to the Model Of Chemistry Considering Aerosols (MOCCA: www.mpch-mainz.mpg.de/~sander/mocca/) results using input data described in case M1 of Table 1b of *Pszenny et al.* [2004]. In the NMT/GT model, Cl is not generated from sea salt aerosol as in the case of the MOCCA model [*Sander and Crutzen*, 1996]; rather, the [Cl] simulated above are used as input to examine the partitioning of Cl species calculated at photostationary state. The amount of Cl flux necessary for the PSS model to maintain photostationary state is added to each model run. Because we do not know the nature of this source (or sources of Cl), we refer to it as the unknown source. It is equal to the washout/rainout and deposition terms of HOCl and HCl. Because there was no precipitate during this flight, the washout/rainout terms were set to 0 s^{-1}. Our estimates of ClO, and HOCl, concentrations are within ~20% of Pszenny et al.'s and are 50% higher for HCl. Our PSS model results are also in good agreement with other clean marine tropical model results (R. von Glasow, personal communication, 2005). Some of the differences are a result of different rate constants and J-values used in the models. The NMT/GT model uses rate constants and photolysis cross-sections recommend by the JPL panel [*Sander et al.*, 2002] and the rate constant for the thermal decomposition of $ClONO_2$ is from *Anderson and Fahey* [1990]. The deposition term for HCl in the NMT/GT model may be too slow in comparison to surface losses used in the M1 case of the MOCCA model.

4. Discussion

[22] The [Cl] time series estimated from our mass balance calculations (Figure 6) has a higher morning concentration that slowly declines to a midday minimum, which is consistent with the buildup of Cl precursors at night [*Keene et al.*, 1990] and a strong midday Cl source [*Knipping et al.*, 2000] or rapid Cl recycling on aerosol particles [*Vogt et al.*, 1996]. The increasing tail after midday in our [Cl] time series (Figure 6) is likely an artifact attributed to the greater variability of the [HO] near the end of the flight (Figure 4) and its impact on the mass balance calculation.

[23] As noted earlier, our PSS model does not simulate Cl production from aerosol. Rather it calculates the amount of

Table 1. First-, Second-, and Third-Order Chlorine Reaction Rates Used in This Study[a]

Number	Process	Rate	Units
R_{Cl} 1	$HO + ClO \rightarrow HCl + O_2$	1.3E-12[b]	cm^3 $molecule^{-1}$ s^{-1}
R_{Cl} 2	$Cl_2 + hv \rightarrow 2Cl$	2.5E-03	s^{-1}
R_{Cl} 3	$Cl + O_3 \rightarrow ClO + O_2$	1.2E-11	cm^3 $molecule^{-1}$ s^{-1}
R_{Cl} 4	$Cl + HO_2 \rightarrow HCl + O_2$	9.1E-12	cm^3 $molecule^{-1}$ s^{-1}
R_{Cl} 5	$Cl + HO_2 \rightarrow HO + ClO$	3.2E-11	cm^3 $molecule^{-1}$ s^{-1}
R_{Cl} 6	$Cl + CH_4 \rightarrow HCl + CH_3$	1.0E-13	cm^3 $molecule^{-1}$ s^{-1}
R_{Cl} 7	$Cl + H_2 \rightarrow HCl + H$	1.6E-14	cm^3 $molecule^{-1}$ s^{-1}
R_{Cl} 8	$Cl + C_2H_6 \rightarrow HCl + C_2H_5$	5.7E-11	cm^3 $molecule^{-1}$ s^{-1}
R_{Cl} 9	$Cl + C_3H_8 \rightarrow HCl + C_3H_7$	1.4E-10	cm^3 $molecule^{-1}$ s^{-1}
R_{Cl} 10	$Cl + H_2CO \rightarrow HCl + HCO$	7.3E-11	cm^3 $molecule^{-1}$ s^{-1}
R_{Cl} 11	$Cl + H_2O_2 \rightarrow HCl + HO_2$	4.1E-13	cm^3 $molecule^{-1}$ s^{-1}
R_{Cl} 12	$Cl + CH_3OOH \rightarrow CH_3O_2 + HCl$	4.0E-11	cm^3 $molecule^{-1}$ s^{-1}
R_{Cl} 13	$Cl + CH_3OOH \rightarrow CH_2O + HO + HCl$	1.7E-11	cm^3 $molecule^{-1}$ s^{-1}
R_{Cl} 14	$Cl + DMS \rightarrow HCl + CH_3SCH_2$	3.3E-10	cm^3 $molecule^{-1}$ s^{-1}
R_{Cl} 15	$Cl + O_2 + M \rightarrow ClOO$	2.7E-33	cm^6 $molecule^{-2}$ s^{-1}
R_{Cl} 16	$ClOO + M \rightarrow Cl + O_2$	1.1E-12	cm^3 $molecule^{-1}$ s^{-1}
R_{Cl} 17	$Cl + ClOO \rightarrow Cl_2 + O_2$	2.3E-10	cm^3 $molecule^{-1}$ s^{-1}
R_{Cl} 18	$Cl + NO + M \rightarrow ClNO + M$	9.1E-32	cm^6 $molecule^{-2}$ s^{-1}
R_{Cl} 19	$ClNO + hv \rightarrow Cl + NO$	3.3E-03	s^{-1}
R_{Cl} 20	$ClNO + Cl \rightarrow Cl_2 + NO$	8.1E-11	cm^3 $molecule^{-1}$ s^{-1}
R_{Cl} 21	$Cl + NO_2 + M \rightarrow ClNO_2 + M$	1.5E-31	cm^6 $molecule^{-2}$ s^{-1}
R_{Cl} 22	$ClNO_2 + hv \rightarrow Cl + NO_2$	3.9E-04	s^{-1}
R_{Cl} 23	$Cl + NO_2 + M \rightarrow ClONO + M$	6.6E-31	cm^6 $molecule^{-2}$ s^{-1}
R_{Cl} 24	$ClONO + hv \rightarrow Cl + NO_2$	4.4E-03	sec^{-1}
R_{Cl} 25	$ClO + NO \rightarrow Cl + NO_2$	1.7E-11	cm^3 $molecule^{-1}$ s^{-1}
R_{Cl} 26	$ClO + HO_2 \rightarrow HOCl + O_2$	5.6E-12	cm^3 $molecule^{-1}$ s^{-1}
R_{Cl} 27	$ClO + ClO \rightarrow Cl + ClOO$	8.1E-15	cm^3 $molecule^{-1}$ s^{-1}
R_{Cl} 28	$ClO + ClO \rightarrow Cl + OClO$	3.5E-15	cm^3 $molecule^{-1}$ s^{-1}
R_{Cl} 29	$ClO + ClO \rightarrow Cl_2 + O_2$	4.8E-15	cm^3 $molecule^{-1}$ s^{-1}
R_{Cl} 30	$ClO + HO \rightarrow HO_2 + Cl$	1.8E-11	cm^3 $molecule^{-1}$ s^{-1}
R_{Cl} 31	$ClO + NO_2 + M \rightarrow ClONO_2$	9.5E-32	cm^6 $molecule^{-2}$ s^{-1}
R_{Cl} 32	$ClONO_2 + hv \rightarrow Cl + NO_3$	4.5E-05	s^{-1}
R_{Cl} 33	$ClONO_2 + hv \rightarrow ClO + NO_2$	9.5E-06	s^{-1}
R_{Cl} 34	$ClONO_2 + Cl \rightarrow Cl_2 + NO_3$	1.0E-11	cm^3 $molecule^{-1}$ s^{-1}
R_{Cl} 35	$ClONO_2 \rightarrow ClO + NO_2$	9.6E-02	s^{-1}
R_{Cl} 36	$OClO + hv \rightarrow ClO + O$	9.6E-02	s^{-1}
R_{Cl} 37	$HOCl + HO \rightarrow ClO + H_2O$	5.6E-13	cm^3 $molecule^{-1}$ s^{-1}
R_{Cl} 38	$HOCl + Cl \rightarrow Cl_2 + HO$	1.9E-12	cm^3 $molecule^{-1}$ s^{-1}
R_{Cl} 39	$HOCl + hv \rightarrow Cl + HO$	3.0E-04	s^{-1}
R_{Cl} 40	$HCl + HO \rightarrow Cl + H_2O$	8.0E-13	cm^3 $molecule^{-1}$ s^{-1}
R_{Cl} 41	$ClO + CH_3OO \rightarrow Cl + HO_2 + HCHO$	2.2E-12	cm^3 $molecule^{-1}$ s^{-1}
R_{Cl} 42	$ClNO_2 + HO \rightarrow HOCl + NO_2$	3.6E-14	cm^3 $molecule^{-1}$ s^{-1}
R_{Cl} 43	deposition HOCl	1.2E-06	s^{-1}
R_{Cl} 44	rainout/Washout HOCl	0	s^{-1}
R_{Cl} 45	deposition HCl	1.2E-05	s^{-1}
R_{Cl} 46	rainout/Washout HCl	0	s^{-1}

[a]The J values were calculated at a solar zenith angle of 30°. Because of the lack of precipitation during this flight, the washout/rainout terms (R_{Cl}43 and R_{Cl}45) were set to 0 s^{-1}. All gas phase constants are from *Sander et al.* [2002]. The deposition rainout/washout rates are adapted from *Davis et al*. [1996].

[b]Read 1.3E-12 as 1.3×10^{-12}.

Cl that must be generated from an unknown source in order to keep the model in steady state based on the [Cl] input into the model (from the mass balance of C_2H_6) and the partitioning of Cl into the inorganic Cl species (i.e., ClO, HOCl, $ClONO_2$, HCl). Thus this source is equal to the sum of the loss process R_{Cl}43 through R_{Cl}46 in Table 1. On average, the unknown source term supplied $\sim 4 \times 10^5$ Cl $cm^{-3}s^{-1}$. This unknown source term can be interpreted as the production of Cl from the photolysis of Cl_2, BrCl, and other photolabile Cl species, produced from (R3) and (R4). Recall that (R4) increases from morning to midday when hydroxyl concentrations peak.

[24] Plots of NMT/GT model output indicate that all Cl containing species have their highest mixing ratios during the early morning (Figure 8). Chlorine mixing ratios (as determined by mass balance) decreased from about 3.4 parts per quadrillion by volume (ppqv) to about 2.3 ppqv during the course of the flight. Early morning mixing ratios of $ClONO_2$ and HOCl are estimated from the PSS model to be $\sim$2.6 and 41 pptv, respectively, decaying to levels of about 2.3 pptv and 26 pptv by 0718 LST. Near noon (1223 LST), $ClONO_2$ and HOCl concentrations appear to have reached minimum mixing ratios of 1.2 and 8 pptv, respectively. Chlorine monoxide concentrations decay in the model simulations from high mixing ratios of $\sim$3 pptv in the morning to levels about half that by midday. Chlorine monoxide concentrations decrease primarily because it partitions quickly with Cl, which decreases by midday. Early morning production of HCl (R_{Cl}4, 6–14) declines primarily in response to the decrease in [Cl] throughout the day. Hydrogen chloride is a relatively long-lived molecule (about 1 day) and is not treated accurately with a photostationary state model. Even so, our noontime [HCl] estimate was only $\sim$50% higher than the MOCCA model test case

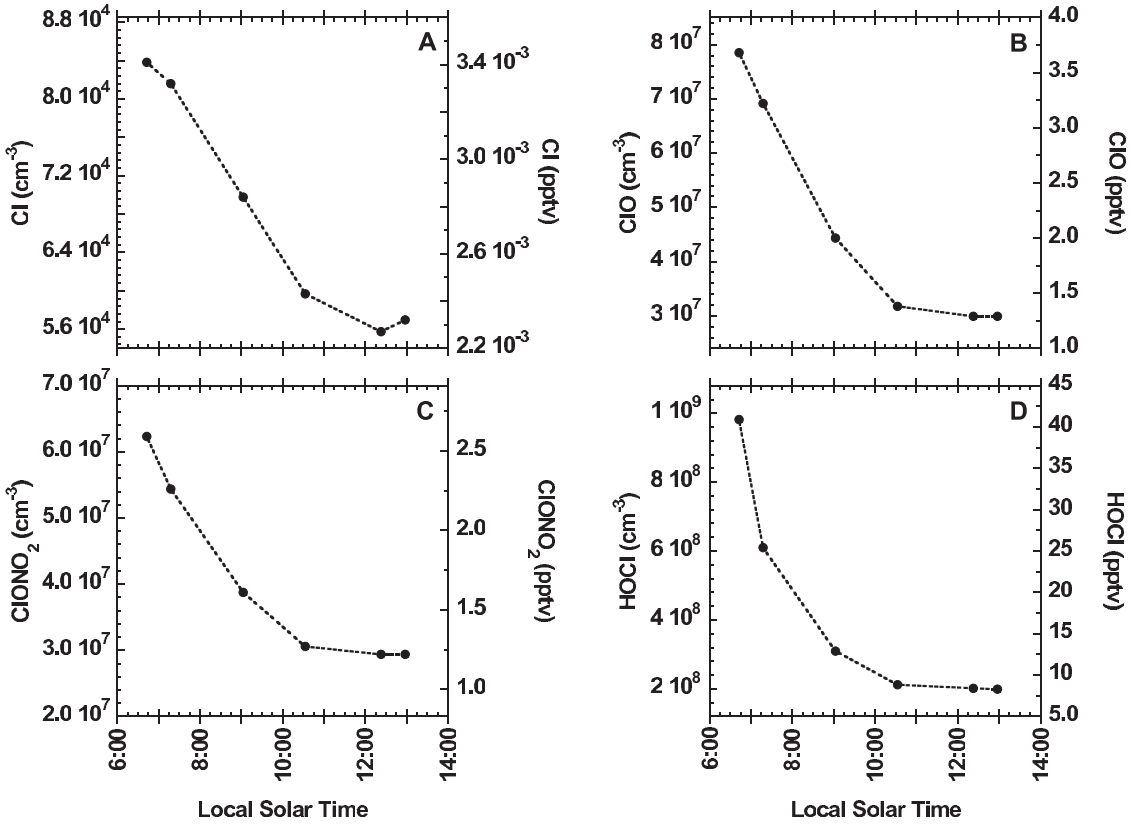

Figure 8. (a) Atomic Cl concentrations derived empirically (see text). These values were used in the NMT/GT PSS model. (b, c, d) Model estimated concentrations of some gas phase inorganic.

for noon. Its abundance is expected to accumulate during the day, while it is being produced, and we estimate that its concentration was about 1 ppbv at noon. Comparison of our model-generated [HO] with measured [HO] is an indication of the accuracy of the model in estimating short-lived species. The modeled [HO] was in excellent agreement with the measured [HO], with the modeled [HO] between 4 and 13% lower than the measured [HO] (Figure 9).

[25] At the beginning of our experiment, 0643 LST, the source of Cl is estimated from the PSS model as coming primarily from an unknown source (~61%), with contributions by HOCl photolysis ($R_{Cl}39$; ~6%), the reaction of $ClO + CH_3O_2$ ($R_{Cl}41$; ~12%), $ClO + NO$ ($R_{Cl}25$; ~9%), and $ClONO_2$ thermal decomposition ($R_{Cl}35$; ~13%) (Table 2).

[26] By 1222 LST, [Cl] dropped merely 30%, indicating that Cl is being produced and/or recycled quickly during the day. A budgetary analysis using the PSS model attributes 41% of the Cl source at midday as coming from the unknown source. Photolysis of HOCl ($R_{Cl}39$), and the reactions $ClO + CH_3O_2$ ($R_{Cl}41$) each contributed about 10% to the [Cl] at midday as estimated during this flight (Table 2). The recycling of Cl via of HCl + HO ($R_{Cl}40$) near noon contributed ~20% to the [Cl]. The importance of HOCl photolysis increases somewhat during the day as its J-value increases and also as the proportion of Cl in this reservoir increases (when HCl is not considered). The contribution of $R_{Cl}39$ as a source increases in importance from about 1% to 20%, as [HO] increase diurnally and the HCl fraction of the total inorganic chlorine concentration grows. The fraction of Cl contributed by $R_{Cl}41$ remains steady throughout the day. Much of the morning CH_3O_2 radical production comes from the abstraction of H from CH_4 by Cl ($R_{Cl}6$) in the presence of O_2 (Table 1).

[27] Our average estimated [Cl*] (the sum of [Cl], [ClO], [Cl_2], [HOCl]) is 4.6×10^8 Cl* cm^{-3}, which is mostly HOCl, is in the middle of the range of mist chamber measurements made in Hawaii (21°22.0′N, 157°42.8′W) during September of 1999 by *Pszenny et al.* [2004] of less than 1.5×10^8 to 9.5×10^8 Cl* cm^{-3}. The present

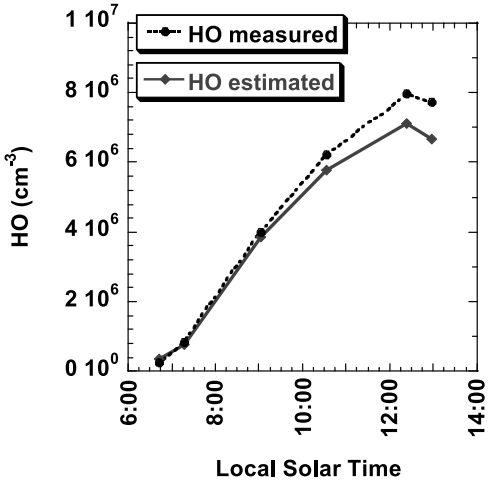

Figure 9. Comparison of measured and model derived HO concentration.

Table 2. Percent Contribution by Reaction to the Source of Cl Per Time of the Flight in Local Solar Time

	Reaction Number	Time					
		0642	0717	0902	1032	1222	1257
Unknown source		61%	58%	48%	45%	41%	43%
HCl + HO	($R_{Cl}40$)	1%	3%	13%	18%	20%	20%
ClO + CH_3O_2	($R_{Cl}41$)	12%	10%	10%	9%	10%	9%
HOCl + hv	($R_{Cl}39$)	6%	7%	10%	10%	11%	10%
ClO + NO	($R_{Cl}25$)	9%	9%	9%	7%	7%	8%
$ClONO_2$ + M	($R_{Cl}35$)	13%	12%	10%	10%	10%	9%

noontime [Cl] estimate of 5.6 (±2.0) × 10^4 Cl cm^{-3} is remarkably similar to our previous noontime estimate [*Wingenter et al.*, 1996] of [Cl] over the North Atlantic near the Azores (~36°N, 21°W) of 6.5 (±1.5) × 10^4 Cl cm^{-3}. This estimate employed hydrocarbon and halocarbon data from flights during the Atlantic Stratocumulus Transition Experiment/Marine Aerosol and Gas Exchange (ASTEX-MAGE) field experiment. However, the Atlantic Lagrangian flights observed an aged continental air mass (which likely influenced the aerosol acidity) and was flown below a stratocumulus layer, which tended to decrease photochemistry in general. Our PEM Tropics A morning estimate [Cl] is also quite comparable to our ASTEX-MAGE estimate. During ASTEX we estimated for one air mass a morning [Cl] of 3.3 (±1.1) × 10^4 Cl cm^{-3} over an 11-hour time period from midnight to 11 a.m. Normalizing this estimate over only the five daylight hours yields a morning average [Cl] of 7.3 (±1.1) × 10^4 Cl cm^{-3} (within errors), nearly identical to our PEM Tropics A morning average of 7.4 (±2.0) × 10^4 Cl cm^{-3}.

[28] A model analysis by *Platt et al.* [2004] needed to invoke a [Cl] of 1.2 to 1.8 × 10^4 Cl cm^{-3} to explain the methane $^{13}C/^{12}C$ ratio in the troposphere of the extra tropical Southern Hemisphere. By contrast, our present estimate of average diurnal [Cl] is ~3.4 × 10^4 Cl cm^{-3}. Because of the assumed lower aerosol pH attributed to higher [DMS] and the increased photochemistry in the tropics, it is reasonable that our average [Cl] should be higher than the *Platt et al.* [2004] estimate. In contrast, our present diurnal average [Cl] is considerably higher than our [Cl] estimate made during the First Aerosol Characterization Experiment (ACE 1) field campaign of 7.2 (±1.0) × 10^2 Cl cm^{-3} [*Wingenter et al.*, 1999]. The ACE 1 estimate was made using data collected on flights over the Southern Ocean when DMS emissions were at a relative low for late spring and aerosol pH was higher [*Hainsworth et al.*, 1998]. It should be noted that our [HO] estimate for ACE 1 [*Wingenter et al.*, 1999] was in excellent agreement with the average photochemically modeled [HO], which was normalized to HO measurements made on the aircraft [*Mauldin et al.*, 1998]. The low average [HO] concentrations (6.1 (±0.3) × 10^5 HO cm^{-3}) estimated during ACE 1 may have also contributed to lower Cl emissions from sea salt aerosols. *Knipping and Dabdub* [2002] derived a linear dependence between the rate of atmospheric Cl_2 formation and gas phase [HO] via (R4).

[29] The difference between our DMS flux estimate (neglecting BrO) of 4.5 (±1.5) × 10^9 DMS m^{-2} s^{-1} and a micro-meteorological approach by *Lenschow et al.* [1999] of 6.1 (±1.9) × 10^9 DMS m^{-2} s^{-1} can be used to infer the average [BrO]. The difference between the two flux estimates, which may not be significant, suggests that an important loss process may have been overlooked in our mass balance analysis, particularly the oxidation of DMS by BrO [*von Glasow and Crutzen*, 2004]. Using equation (5) and increasing the flux term to the estimate of Lenschow et al., the minimum in chi-square occurs when the average BrO mixing ratio is 1.3 (±1.3) pptv. The photolysis of bromoform ($CHBr_3$) at noon, with a mixing ratio of 4.5 pptv, would only have provided about 0.01% of the Br source.

[30] In the work of *Pszenny et al.* [2004], a BrO mixing ratio of 0.3 pptv was estimated from relative changes in the BrO signal of the DOAS instrument, although the measured BrO was never above the detection limit of 2 pptv during the Hawaii experiment. The tropospheric "background" mixing ratio is estimated to be 1–2 pptv [*Fitzenberger et al.*, 2000]. Thus our BrO estimate of 1.3 (±1.3) pptv, with its large uncertainty, is within the range of these observations.

[31] It is estimated that over the course of the flight, approximately 44% of the DMS was oxidized by HO and 56% by Cl, when only these two oxidants are taken into account (Table 3). When 1.3 pptv of BrO is also considered, it is estimated that HO oxidized 33% of the DMS, while chlorine oxidized 41%, and BrO 26% (Table 3). At these temperatures (approximately 298 K) much of the HO oxidation proceeds by H abstraction [*Davis et al.*, 1999] and about half of the oxidation of DMS by Cl is by hydrogen abstraction. However, addition of BrO to DMS leads to the formation of DMSO [*Ingham et al.*, 1999; *von Glasow and Crutzen*, 2004]. The DMSO channel leads mainly to particle growth, whereas H abstraction has a greater probability of forming new particles. Therefore knowledge of the type and abundance of halogen chemistry that is present is important in the understanding of key processes that determine the radiative budget of the Earth.

5. Conclusion

[32] Atomic chlorine concentrations were estimated during a Lagrangian flight near Christmas Island using measurements of [HO] and [C_2H_6] and were found to be 8.4 (±2.0) × 10^4 Cl cm^{-3} in the early morning, decreasing about 30% to 5.7 (±2.0) × 10^4 Cl cm^{-3} at midday. This diurnal change can be attributed to the buildup of Cl precursors overnight and efficient heterogeneous generation or regeneration of photolabile chlorine species from aerosol. Because of the associated uncertainty, mostly from the mixing term, the actual Cl diurnal profile may deviate from that determined using mass balance. The [Cl] time series derived above served as an input in our PSS model used to demonstrate the potential partitioning of inorganic chlorine species within the limitations of this type of model. The empirically derived [Cl] time series was also used in another mass balance analysis yielding a DMS flux estimate of 4.5 (±1.5) × 10^9 DMS m^{-2} s^{-1}. This flux estimate was found

Table 3. Percent Oxidation of DMS in Cases 1 and 2

	Case 1	Case 2
HO	44%	33%
Cl	56%	41%
BrO[a]		26%

[a]Considered at 1.3 pptv.

to be a factor of 2 higher than when HO is the only oxidant considered in such calculations [*Davis et al.*, 1999]. Comparison of this DMS flux with that of another DMS flux estimate, employing a micro-meteorological technique [*Lenschow et al.*, 1999], indicated another loss term may be needed in our mass balance approach, although the differences between the two estimates may not be significant. In order to minimize differences between our DMS flux estimates and that of Lenschow et al.'s, we postulate that an average BrO mixing ratio of 1.3 (±1.3) pptv must be present. When considering all three oxidants, 33% of the DMS was oxidized by HO, 41% by Cl, and 26% by BrO. Oxidation of DMS and subsequent formation of new particles or growth of existing particles is not only temperature dependent but also oxidant dependent. Accurate knowledge of the flux of DMS and type and quantity of oxidants present is needed to better understand the impact of the DMS on particle formation, growth, and the radiative properties of the Earth.

[33] **Acknowledgments.** Data were provided by Fred Eisele, Lee Mauldin, Alan Bandy, and Don Thornton. Gao Chen, Jim Crawford, and Doug Davis contributed to the development of the PSS model and provided valuable discussions. Don Lenschow and Tim Bates also contributed with valuable discussions. We would like to express our appreciation to the excellent team at UCI, who worked hard in the laboratory, at the computer, and in the field to produce this NMHC and halocarbon data set, especially Doug Begbie, John Bilicska, Tai-Yih Chen, Nancy Conebeare, David Crosley, Kathy Farrow, Mike Gilligan, Adam Hill, Melissa Hill, Jenn Lapierre, Stacey Lasswell, Jan Latour, Brent Love, Geoff Luke, Murray McEachern, Russell Miller, Christina Rekaski, and Nick Shiavone. We are also grateful to Barbara Yu and Wynn Norris for their assistance during the project. This work is part of the Halogens in the Troposphere (HitT) and Surface Ocean Lower Atmosphere (SOLAS) initiatives. The PEM-Tropics A research was supported by the NASA Global Tropospheric Chemistry Experiment Program, grants NAG-1-1777 and NAG-1-1769.

References

Anderson, L. C., and D. W. Fahey (1990), Studies with $ClONO_2$: Thermal dissociation rate and catalytic conversion to NO using an NO/O_3 chemiluminescence detector, *J. Phys. Chem.*, *99*, 644–652.

Abbatt, J. P. D., and G. C. G. Waschewsky (1998), Heterogeneous interactions of HOBr, HNO_3, O_3 and NO_2 with deliquescent NaCl aerosols at room temperature, *J. Phys. Chem. A*, *102*, 3719–3725.

Archer, S. D., C. E. Stelfox-Widdicombe, P. H. Burkill, and G. Malin (2001), A dilution approach to quantify the production of dissolved dimethylsulphoniopropionate and dimethyl sulphide due to microzooplankton herbivory, *Aquat. Microb. Ecol.*, *23*, 131–145.

Ariya, P. A., B. T. Jobson, R. Sander, H. Niki, G. W. Harris, J. F. Hopper, and K. G. Anlauf (1998), Measurements of C_2–C_7 hydrocarbons during the Polar Sunrise Experiment 1994: Further evidence for halogen chemistry in the troposphere, *J. Geophys. Res.*, *103*, 13,169–13,180.

Avallone, L. M., D. W. Toohey, T. J. Fortin, K. A. McKinney, and J. D. Fuentes (2003), In situ measurements of bromine oxide at two high-latitude boundary layer sites: Implications of variability, *J. Geophys. Res.*, *108*(D3), 4089, doi:10.1029/2002JD002843.

Bates, T. S., R. J. Charlson, and R. H. Gammon (1987a), Evidence for the climatic role of marine biogenic sulfur, *Nature*, *329*, 319–321.

Bates, T. S., J. D. Cline, R. H. Gammon, and S. R. Kelly-Hansen (1987b), Regional and seasonal variations in the flux of oceanic dimethylsulfide to the atmosphere, *J. Geophys. Res.*, *92*, 2930–2938.

Blake, N. J., et al. (1999), Influence of Southern Hemispheric biomass burning on mid-tropospheric distributions of nonmethane hydrocarbons and selected halocarbons over the remote South Pacific, *J. Geophys. Res.*, *104*, 16,213–16,232.

Bradshaw, J., et al. (1999), Photofragmentation two-photon laser-induced fluorescence detection of NO_2 and NO: Comparison of measurements with model results based on airborne observations during PEM-Tropics A, *Geophys. Res. Lett.*, *26*, 471–474.

Cantrell, C. A., R. E. Shetter, A. H. McDaniel, J. G. Calvert, J. A. Davidson, D. C. Lowe, S. C. Tyler, R. J. Cicerone, and J. P. Greenberg (1990), Carbon kinetic isotope effect in the oxidation of methane by the hydroxyl radical, *J. Geophys. Res.*, *95*, 22,455–22,462.

Charlson, R. J., J. E. Lovelock, M. O. Andreae, and S. G. Warren (1987), Oceanic phytoplankton, atmospheric sulfur, cloud albedo, and climate, *Nature*, *326*, 655–661.

Chin, M., D. L. Savoie, B. J. Huebert, A. R. Bandy, D. C. Thornton, T. S. Bates, P. K. Quinn, E. S. Saltzman, and W. J. De Bruyn (2000), Atmospheric sulfur cycle simulated in the global model GOCART: Comparison with field observations and regional budgets, *J. Geophys. Res.*, *105*, 24,689–24,712.

Clarke, A. D., et al. (1998), Particle nucleation in the tropical boundary layer and its coupling to marine sulfur sources, *Science*, *282*, 89–92.

Davis, D., J. Crawford, S. Liu, S. McKeen, A. Bandy, D. Thornton, F. Rowland, and D. Blake (1996), Potential impact of iodine on tropospheric levels of ozone and other critical oxidants, *J. Geophys. Res.*, *101*, 2135–2147.

Davis, D., et al. (1999), Dimethyl sulfide oxidation in the equatorial Pacific: Comparison of model simulations with field observations for DMS, SO_2, H_2SO_4(g), MSA(g), MS, and NSS, *J. Geophys. Res.*, *104*, 5765–5784.

Duce, R. A., J. T. Wasson, J. W. Winchester, and F. Burns (1963), Atmospheric iodine, bromine, and chlorine, *J. Geophys. Res.*, *68*, 3943–3947.

Fickert, S., J. W. Adams, and J. N. Crowley (1999), Activation of Br_2 and BrCl via uptake of HOBr onto aqueous salt solutions, *J. Geophys. Res.*, *104*, 23,719–23,727.

Finlayson-Pitts, B. J. (2003), The tropospheric chemistry of sea salt: A molecular-level view of the chemistry of NaCl and NaBr, *Chem. Rev.*, *103*, 4801–4822.

Fitzenberger, R., H. Bösch, C. Camy-Peyret, M. P. Chipperfield, H. Harder, and U. Platt (2000), First profile measurements of tropospheric BrO, *Geophys. Res. Lett.*, *27*, 2921–2924.

Hainsworth, A. H. W., A. L. Dick, and J. L. Gras (1998), Climatic context of the First Aerosol Characterization Experiment (ACE 1): A meteorological and chemical overview, *J. Geophys. Res.*, *103*, 16,319–16,340.

Hausmann, M., and U. Platt (1994), Spectroscopic measurements of bromine oxide and ozone in the high Arctic during Polar Sunrise Experiment 1992, *J. Geophys. Res.*, *99*, 25,399–25,413.

Hebestreit, R. M., J. Stutz, D. Rosen, V. Matveev, M. Luria, and U. Platt (1999), DOAS measurements of tropospheric bromine oxide in mid-latitudes, *Science*, *283*, 55–57.

Hegels, E., P. J. Crutzen, T. Klüpfel, D. Perner, and J. P. Burrows (1998), Global distribution of atmospheric bromine oxide from GOME on the earth observing satellite ERS-2, *Geophys. Res. Lett.*, *25*, 3127–3139.

Hoell, J. M., D. D. Davis, D. J. Jacob, M. O. Rodgers, R. E. Newell, H. E. Fuelberg, R. J. McNeal, J. L. Raper, and R. J. Bendura (1999), Pacific Exploratory Mission in the tropical Pacific: PEM-Tropics A, August–September 1996, *J. Geophys. Res.*, *104*, 5567–5583.

Ingham, T., D. Bauer, R. Sander, P. J. Crutzen, and J. N. Crowley (1999), Kinetics and products of the reactions BrO+DMS and Br+DMS at 298 K, *J. Phys. Chem. A*, *103*, 7199–7209.

Jobson, B. T., H. Niki, Y. Yokouchi, J. Bottenheim, F. Hopper, and R. Leaitch (1994), Measurements of C2–C6 hydrocarbons during the Polar Sunrise 1992 Experiment: Evidence for Cl atom and Br atom chemistry, *J. Geophys. Res.*, *99*, 25,355–25,368.

Keene, W. C., A. A. P. Pszenny, D. J. Jacob, R. A. Duce, J. N. Galloway, J. J. Schultz-Tokos, H. Sievering, and J. F. Boatman (1990), The geochemical cycling of reactive Cl through the marine troposphere, *Global Biogeochem. Cycles*, *4*, 407–430.

Keller, M. D., W. K. Bellows, and R. L. Guillard (1989), Dimethylsulfide production in marine phytoplankton, in *Biogenic Sulfur in the Environment*, edited by E. S. Saltzman and W. J. Cooper, pp. 167–182, Am. Chem. Soc., Washington, D. C.

Knipping, E. M., and D. Dabdub (2002), Modeling study of Cl_2 formation by interfacial reactions of OH and Cl^- on deliquesced NaCl particles, *J. Geophys. Res.*, *107*(D18), 4360, doi:10.1029/2001JD000867.

Knipping, E. M., and D. Dabdub (2003), Impact of chlorine emissions from sea-salt aerosol on coastal urban ozone, *Environ. Sci. Technol.*, *37*, 275–284.

Knipping, E. M., M. J. Lakin, K. L. Foster, P. Jungwirth, D. J. Tobias, R. B. Gerber, D. Dabdub, and B. J.. Finlayson-Pitts (2000), Experiments and molecular/kinetics simulations of ion-enhanced interfacial chemistry on aqueous NaCl aerosols, *Science*, *288*, 301–306.

Lenschow, D. H., I. R. Paluch, A. R. Bandy, D. C. Thornton, D. R. Blake, and I. Simpson (1999), Use of a mixed-layer model to estimate dimethylsulfide flux and application to other trace gas fluxes, *J. Geophys. Res.*, *104*, 16,275–16,295.

Mauldin, R. L., III, G. J. Frost, G. Chen, D. J. Tanner, A. S. H. Prévôt, D. D. Davis, and F. L. Eisele (1998), OH measurements during the First Aerosol Characterization Experiment (ACE 1): Observations and model comparisons, *J. Geophys. Res.*, *103*, 16,713–16,729.

Mauldin, R. L., III, D. J. Tanner, and F. L. Eisele (1999), Measurements of OH during PEM-Tropics A, *J. Geophys. Res.*, *104*, 5817–5828.

Oum, K., M. J. Lakin, D. O. De Haan, T. Brauers, and B. J. Finlayson-Pitts (1998), Formation of molecular chlorine from the photolysis of ozone and aqueous sea-salt particles, *Science*, *279*, 74–77.

Platt, U., W. Allan, and D. Lowe (2004), Hemispheric average Cl atom concentration from C^{13}/C^{12} ratios in atmospheric methane, *Atmos. Chem. Phys. Discuss.*, *4*, 2393–2399.

Pszenny, A. A. P., J. Moldanová, W. C. Keene, R. Sander, J. R. Maben, M. Martinez, P. J. Crutzen, D. Perner, and R. G. Prinn (2004), Halogen cycling and aerosol pH in the Hawaiian marine boundary layer, *Atmos. Chem. Phys. Discuss.*, *3*, 4701–4753.

Ragains, M. L., and B. J. Finlayson-Pitts (1997), Kinetics and mechanism of the reaction of Cl atoms with 2-methyl-1, 3-butadiene (isoprene) at 298 K, *J. Phys. Chem. A*, *101*, 1509–1517.

Ramacher, B., J. Rudolph, and R. Koppmann (1999), Hydrocarbon measurements during tropospheric ozone depletion events: Evidence for halogen atom chemistry, *J. Geophys. Res.*, *104*, 3633–3653.

Rossi, M. J. (2003), Heterogeneous reactions on salts, *Chem. Rev.*, *103*, 4823–4882.

Sander, R., and P. J. Crutzen (1996), Model study indicating halogen activation and ozone destruction in polluted air masses transported to the sea, *J. Geophys. Res.*, *101*, 9121–9138.

Sander, R., R. Vogt, G. W. Harris, and P. J. Crutzen (1997), Modelling the chemistry of ozone, halogen compounds, and hydrocarbons in the arctic troposphere during spring, *Tellus, Ser. B*, *49*, 522–532.

Sander, S. P., et al. (2002), Chemical kinetics and photochemical data for use in atmospheric studies, *JPL Pub. 02-25*.

Saueressig, G., P. Bergamaschi, J. Crowley, C. Brühl, H. Fischer, and G. W. Harris (1995), Carbon kinetic isotope effect in the reaction of CH_4 and Cl atoms, *Geophys. Res. Lett.*, *22*, 1225–1228.

Saueressig, G., J. Crowley, P. Bergamaschi, C. Brühl, C. A. M. Brenninkmeijer, and H. Fischer (2001), $^{13}C/^{12}C$ and D/H kinetic isotope effects in the reactions of CH^4 with $O(^1D)$ and OH: New laboratory measurements and their implications for the isotopic composition of stratospheric methane, *J. Geophys. Res.*, *106*, 23,127–23,138.

Singh, H. B., and J. F. Kasting (1988), Chlorine-hydrocarbon photochemistry in the marine troposphere and lower stratosphere, *J. Atmos. Chem.*, *7*, 261–285.

Singh, H. B., et al. (1996), Low ozone in the marine boundary layer of the tropical Pacific Ocean: Photochemical loss, chlorine atoms, and entrainment, *J. Geophys. Res.*, *101*, 1907–1917.

Spicer, C. W., E. G. Chapman, B. J. Finlayson-Pitts, R. A. Plastridge, J. M. Hubbe, J. D. Fast, and C. M. Berkowitz (1998), Unexpectedly high concentrations of molecular chlorine in coastal air, *Nature*, *394*, 353–356.

Stickel, R. E., J. M. Nicovich, S. Wang, Z. Zhao, and P. H. Wine (1992), Kinetic and mechanistic study of the reaction of atomic chlorine with dimethyl sulfide, *J. Phys. Chem.*, *96*, 9875–9883.

Stutz, J., R. Ackermann, J. D. Fast, and L. Barrie (2002), Atmospheric reactive chlorine and bromine at the Great Salt Lake, Utah, *Geophys. Res. Lett.*, *29*(10), 1380, doi:10.1029/2002GL014812.

Tanaka, P. L., et al. (2003), Direct evidence for chlorine-enhanced urban ozone formation in Houston, Texas, *Atmos. Environ.*, *37*, 1393–1400.

Tyler, S. C., H. O. Ajie, A. L. Rice, R. J. Cicerone, and E. C. Tuazon (2000), Experimentally determined kinetic isotope effects in the reaction of CH_4 with Cl: Implications for atmospheric CH_4, *Geophys. Res. Lett.*, *27*, 1715–1718.

Urbanski, S. P., and P. H. Wine (1999), Spectroscopic and kinetic study of the Cl-$S(CH_3)_2$ adduct, *J. Phys. Chem. A*, *103*, 10,945–10,954.

Vogt, R., P. J. Crutzen, and R. Sander (1996), A mechanism for halogen release from sea-salt aerosol in the remote marine boundary layer, *Nature*, *383*, 327–330.

von Glasow, R., and P. J. Crutzen (2003), Tropospheric halogen chemistry, in *Treatise on Geochemistry*, edited by K. K. Turekian and H. D. Holland, pp. 21–64, Yale Univ. Press, New Haven, Conn.

von Glasow, R., and P. J. Crutzen (2004), Model study of multiphase DMS oxidation with a focus on halogens, *Atmos. Chem. Phys.*, *4*, 589–608.

Wagner, T., C. Leue, M. Wenig, K. Pfeilsticker, and U. Platt (2001), Spatial and temporal distribution of enhanced boundary layer BrO concentrations measured by the GOME instrument aboard ERS-2, *J. Geophys. Res.*, *106*, 24,225–24,236.

Wingenter, O. W., M. K. Kubo, N. J. Blake, T. W. Smith Jr., D. R. Blake, and F. S. Rowland (1996), Hydrocarbon and halocarbon measurements as photochemical and dynamical indicators of atmospheric hydroxyl, atomic chlorine, and vertical mixing obtained during Lagrangian flights, *J. Geophys. Res.*, *101*, 4331–4340.

Wingenter, O. W., D. R. Blake, N. J. Blake, B. C. Sive, and F. S. Rowland (1999), Tropospheric hydroxyl and atomic chlorine concentrations, and mixing timescales determined from hydrocarbon and halocarbon measurements made over the Southern Ocean, *J. Geophys. Res.*, *104*, 21,819–21,828.

Wingenter, O. W., B. C. Sive, D. R. Blake, F. S. Rowland, and B. A. Ridley (2003), Unexplained enhancements of CH_3Br in the Arctic and sub-Arctic lower troposphere during TOPSE spring 2000, *Geophys. Res. Lett.*, *30*(22), 2160, doi:10.1029/2003GL018159.

Wingenter, O. W., K. B. Haase, P. Strutton, G. Friederich, S. Meinardi, D. R. Blake, and F. S. Rowland (2004), Changing concentrations of CO, CH_4, C_5H_8, CH_3Br, CH_3I, and dimethyl sulfide during the Southern Ocean Iron Enrichment Experiments, *Proc. Natl. Acad. Sci. U. S. A.*, *101*, 8537–8541, doi:10.1073/pnas.0402744101.

O. W. Wingenter, Department of Chemistry and Geophysical Research Center, New Mexico Institute of Mining and Technology, Socorro, NM 87801, USA. (oliver@nmt.edu)

D. R. Blake, N. J. Blake, and F. S. Rowland, Department of Chemistry, University of California, Irvine, CA 92697, USA.

B. C. Sive, CCRC-ISEOS, University of New Hampshire, Durham, NH 03824, USA.